Global journal of multidisciplinary and applied sciences

Available online at www.gjmas.net

©2020 GJMAS Journal-2020-5-1/1-12

ISSN **2313-6685** ©2020 GJMAS

Analyzing the evolution of actual evolution and predicting its future status Haji Ghoshan watershed

Rouhollah Sheikh[1], Esmaeil Shahkooeei[2*] and Abdul Azim Ghankarmaee[2]

1. Master of Science in Climatology, Golestan University Iran
2. Assistant Professor, Faculty of Humanities, Golestan University, Iran

***Corresponding author*:** Esmaeil Shahkooeei

ABSTRACT: Evaporation is one of the important factors in the hydrological cycle and is one of the determinants of energy equilibrium at ground level and water balance, and its estimation is required in various fields such as hydrology, agriculture, forest management and pasture management, and water resource management. 44% of the precipitation is due to evaporation from the surface of the earth. In fact, evaporation is the cause of the relationship between the important elements of the planet and the atmosphere. However, one of the concerns of authorities in the water sector is the availability of evapotranspiration data that can properly monitor the conditions. But unfortunately, the access to experimental data of the Lysymeter device is very limited and its statistical period is negligible. Therefore, the present study, based on the Toronto White water bill, predicts the actual evaporation of the Haji Ghoshan watershed for two bases (1350 to 1390) and the future (1391 to 1428) using the results of the GISS general circulation model and the two scenarios of change The climate of RCP4.5 and RCP8.5 has been analyzed. To this end, we tried to simulate the current status and future condition of the four components of the temperature, and analyze the potential and probabilistic data in two basic periods of simulation. However, in the present study, the comparison with the RCP8.5 and RCP4.5 scenarios for the base period from baseline between 1351 to 1390 and the upcoming period between 1391 and 1430, in both scenarios in The future will have a significant decline compared to the actual evaporation base, and in spite of this, potential evaporation will increase dramatically in the studied area.

***Keywords*:** Real evaporation, Rcp, Haji Ghoshan.

INTRODUCTION

Evaporation is one of the important factors in the hydrological cycle and is one of the determinants of energy equilibrium at ground level and water balance, and its estimation is required in various fields such as hydrology, agriculture, forest and pasture management, and water resource management. 44% of the precipitation is due to evaporation from the surface of the earth. In fact, evaporation causes the connection between the important elements of the planet and the atmosphere. (Su et al., 2004). Among the various processes of the hydrological cycle, the actual evaporation measure is the most difficult of them (Alizadeh, 2002). In evolution hydrography engineering, it is important from two directions: First, evaporation from rivers, lakes and reservoirs of dams causes water losses that need to be calculated, second, evaporation from the soil surface and vegetation in the watersheds is one of the components The water cycle is considered. Due to the significant changes in the components of the hydrological cycle in the time and place scale, knowing the key components controlling the temporal and spatial variations of the surface water bill, especially in arid and semi arid regions, is very important. Evapotranspiration is related to water and soil balance and plays a key role in climate-soil-vegetation interactions (2007, Yang). Evapotranspiration is one of the most important ways of using or wasting water in a watershed, which monitoring and evaluating its changes over time can be used to indicate the amount of water consumed in each land use, in water management in the scale of the area, and to determine the extent The water needed to be allocated to any land use is to be used. The amount of explanation coefficients ranged from 0.15 to 0.99 in all of the parameters in their research, which indicates the high capability of the sandal algorithm for calculating

evapotranspiration. Georges et al. (2008) evaluated the actual evapotranspiration obtained from the sandal algorithm in images from aerial platforms in the state of Texas, using lysymmetric data. The magnitude of the squared error obtained from the Sahal algorithm from this study was 0.15 mm per day. In Iran, Hamid Gholizadeh's studies on the study of time variation of potential evapotranspiration in Tabriz using the Blanie Crydell method concluded that, despite the slowdown of this index until the 1990s, gradually evolved over the past few years, the potential for increase Finding the temporal and spatial variation of the temporal and spatial variation of the coefficient of evaporation in Kermanshah province, conducted by Maryam Ahmadi in 2011, and the results of this study showed that the amount of seasonal tidal force in summer is the lowest and in autumn and spring, it has higher values. Meanwhile, the results indicated that the value of the trough coefficient is inverse with the height from the sea level. , The maximum increase in evapotranspiration is in mid-spring and autumn, and monthly changes in this index show a significant increase for the months of May and October, while evaporation-potential currents in most of the summer months (July, August, September) Despite the high fluctuation, the trend shows a non-significant trend. The daily and monthly evapotranspiration rates for Kermanshah station were compared with the obtained coefficients by the methodology proposed by the World Food and Agriculture Organization (FAO). Although the correlation between daily results was not high, but the monthly coefficients were high correlated, in a study to determine and evaluate actual evapotranspiration using remote sensing data on Golestan Surrender Basin, by Mir Hossein Miriqoubzadeh et al, 2013.

Data and methods

Introduction of Exposure Microscopicity of precipitation and temperature in Golestan Province watersheds

At first, a monthly rainfall and temperature data series for the years 1971 to 2011 was designed to simulate and fine-scale the scale of these two components for decades to come. Subsequently, data from the NASA Meteorological Center (thredds-ncss-grid-CMIP5) related to the predictive components of the GISS General Flow Model for the range of 35 to 50 degrees north and 50 to 60 degrees east. The predictive components of the GISS model include 81 general atmospheric components whose resolution is 2.5 × 2.5 degrees degrees longitude and latitude (Table 1). For the purpose of preliminary and fine-scale observation of the rainfall and temperature data of the study basin, the best correlations between the turning points for the base period were used, which covers the years 1971 to 2011, and then for training and testing, the period The base was separated from 1971 to 2006 and 2006 to 2011. Finally, according to the parametric correlation method (Pearson), the relations were evaluated and then the modeling results were verified based on the coefficients of determining and testing the residue independence based on Watson's camera method. Therefore, based on the lowest error in modeling, it was found that the best relationship between the components of the geopotential heights and the vertical wind (omega (= dp / dt)) has been achieved at three levels of 850, 700 and 500 hPa. These components were used to predict the precipitation and temperature of the coming decades.

Table 1. 81 Predictive Component of the GISS General Flow Model

Row	Turning component	Row	Turning component
1	zg = Geopotential Height	42	ra = Carbon Mass Flux into Atmosphere due to Autotrophic (Plant) Respiration on Land
2	wap = omega (=dp/dt)	43	psl = Sea Level Pressure
3	vo = Sea Water Y Velocity	44	ps = Surface Air Pressure
4	vas = Northward Near-Surface Wind	45	prw = Water Vapor Path
5	va = Northward Wind	46	prveg = Precipitation onto Canopy
6	uo = Sea Water X Velocity	47	prsn = Snowfall Flux
7	uas = Eastward Near-Surface Wind	48	prc = Convective Precipitation
8	ua = Eastward Wind	49	pr = Precipitation
9	tsl = Temperature of Soil	50	npp = Carbon Mass Flux out of Atmosphere due to Net Primary Production on Land
10	ts = Surface Temperature	51	nep = Net Carbon Mass Flux out of Atmophere due to Net Ecosystem Productivity on Land.
11	transiy = Y-Component of Sea Ice Mass Transport	52	mrsos = Moisture in Upper Portion of Soil Column
12	transix = X-Component of Sea Ice Mass Transport	53	mrso = Total Soil Moisture Content
13	tran = Transpiration	54	mrros = Surface Runoff
14	tos = Sea Surface Temperature	55	mrso = Total Soil Moisture Content
15	thetao = Sea Water Potential Temperature	56	mrro = Total Runoff
16	tauv = Surface Downward Northward Wind Stress	57	mrlsl = Water Content of Soil Layer
17	tauu = Surface Downward Eastward Wind Stress	58	mrfso = Soil Frozen Water Content
18	tasmin = Daily Minimum Near-Surface Air Temperature	59	mc = Convective Mass Flux
19	tasmax = Daily Maximum Near-Surface Air Temperature	60	huss = Near-Surface Specific Humidity
20	tas = Near-Surface Air Temperature	61	hus = Specific Humidity
21	ta = Air Temperature	62	hurs = Near-Surface Relative Humidity
22	sos = Sea Surface Salinity	63	hur = Relative Humidity
23	so = Sea Water Salinity	64	hfss = Surface Upward Sensible Heat Flux
24	snw = Surface Snow Amount	65	hfls = Surface Upward Latent Heat Flux

25	snm = Surface Snow Melt	66	gpp = Carbon Mass Flux out of Atmosphere due to Gross Primary Production on Land
26	snd = Snow Depth	67	evspsblveg = Evaporation from Canopy
27	snc = Snow Area Fraction	68	evspsblsoi = Water Evaporation from Soil
28	sit = Sea Ice Thickness	69	evspsbl = Evaporation
29	sic = Sea Ice Area Fraction	70	evap = Water Evaporation Flux from Sea Ice
30	sfcWind = Near-Surface Wind Speed	71	clwvi = Condensed Water Path
31	sci = Fraction of Time Shallow Convection Occurs	72	clw = Mass Fraction of Cloud Liquid Water
32	sbl = Surface Snow and Ice Sublimation Flux	73	clt = Total Cloud Fraction
33	rtmt = Net Downward Flux at Top of Model	74	clivi = Ice Water Path
34	rsutcs = TOA Outgoing Clear-Sky Shortwave Radiation	75	cli = Mass Fraction of Cloud Ice
35	rsut = TOA Outgoing Shortwave Radiation	76	cl = Cloud Area Fraction
36	rsuscs = Surface Upwelling Clear-Sky Shortwave Radiation	77	ci = Fraction of Time Convection Occurs
37	rsus = Surface Upwelling Shortwave Radiation	78	cct = Air Pressure at Convective Cloud Top
38	rlus = Surface Upwelling Longwave Radiation	79	ccb = Air Pressure at Convective Cloud Base
39	rldscs = Surface Downwelling Clear-Sky Longwave Radiation	80	cSoil = Carbon Mass in Soil Pool
40	rlds = Surface Downwelling Longwave Radiation	81	baresoilFrac = Bare Soil Fraction
41	rh = Carbon Mass Flux into Atmosphere due to Heterotrophic Respiration on Land	-	-

Since the purpose of this study is to prepare a real evaporation map on a monthly basis, it was therefore necessary to use the data of the average monthly precipitation (P) and temperature (T), respectively, 7 evapotranspiration and potential (PET) evapotranspiration and Actual transpiration (AET), available plant root water (PAW), soil moisture storage (DS), surplus, deficit deficiency) are calculated in Excel. It is worth noting that the estimation and calculation of some of the components used in this research is dependent on the soil type of the region, which will be referred to below. Therefore, in the first step of the blue-billed model, it is necessary to calculate potential).evapotranspiration values for each of the months of the year using the Torrent White method (Alizadeh, 2006:

A. First, the thermal profile (Im) is calculated for each of the months of the year (1):

Relationship (1): $\mathrm{Im} = \left(\frac{Tm}{5}\right) 1.5$

In this regard, the Im equation is the thermal profile of each month and Tm is the average temperature of the month in question. This is done for all 12 months of the year. If the average temperature is zero or negative in a month, Im is considered zero for that month (Mahdavi, 1392)

B- The thermal profile of year (I) will be calculated from the sum of monthly heat profiles during the year through relation (2) (Mahdavi, 1392)

Relation (2): $\mathrm{I} = \sum_{n=1}^{12} im$

C: With annual thermal profile (I), coefficient a is calculated from (Mahdavi, 1392).

Relation (3): $a=(6.75*6.75 * 10^{-7})\ \mathrm{I}^3-(7.71 * 10^{-5})\mathrm{I}^2 + (1.792 * 10^{-2})\mathrm{I} + 0.492$

D) For each of the months of the year, the potential evapotranspiration in millimeters is calculated from Equation (4) (Alizadeh, 2006)

Relationship (4): $\mathrm{PET} = (\frac{10\ \mathrm{Tm}}{\mathrm{I}})\ \mathrm{a}$

E) Potential evapotranspiration must be corrected by applying Nm coefficient for different months. Therefore, the calculation of potential evapotranspiration from equation (5) is as follows (Mahdavi, 1392)

Relation(5): $\mathrm{PET} = 16\ \mathrm{Nm}(\frac{10\ \mathrm{Tm}}{\mathrm{I}})\mathrm{a}$

In the second step, modeling the water balance of the studied basin, the actual evapotranspiration (AET) calculation is required in order to obtain its value from the following conditional rules using relations (6) and (7)

Relation (6): $\mathrm{IF}\ [(\mathrm{P}) > (\mathrm{PET}); \mathrm{PET} = \mathrm{AET}]$

Relationship (7): $\mathrm{IF}\ [(\mathrm{P}) \leq (\mathrm{PET}); \mathrm{PAW(n)} + \mathrm{P(o)}]$

In the above relations, real evapotranspiration is calculated according to the amount of precipitation (P) and potential evapotranspiration (PET) of the current month and soil moisture conditions in the previous month. Therefore, using the condition rule, if the rainfall is greater than potential evapotranspiration (PET), then the AET will be equal to the PET value and if the amount of precipitation is equal to or smaller than potential evapotranspiration (PET), the numerical value of water The available plant root (PAW) will be collected in the previous month with the current month's rainfall, and the resulting value will be equal to the AET. As specified in conditional relation (7), a component called the available plant root water (PAW)

Has been talked about. In order to calculate maximum plant water (PAWMAX) and available plant root water (PAW), relations (8) and (9) were used:

Relationship (8): $PAW_{MAX}=(FC-PWP)*z$
Relationship (9): $PAW= Z*1000*(FC-PWP)$

In the above relation, FC is the permeability potential of the earth, PWP is the wilting point, the values of these two components are derived based on the different type of soil from Table (2), also the Z component is the depth of the root, for the study area its coefficient is 0.6 opnions have been asked.

Table 2. Determination of FC and PWP coefficients based on soil texture types

Texture	FC	PWP
Clay	0.3	0.15
Clay Loam	0.25	0.12
Loam	0.2	0.1
Sandy Loam	0.12	0.05
Sand	0.09	0.02

In order to calculate the excess water, soil moisture storage changes (DS) must be calculated first. Therefore, in order to calculate the value of this component, relation (10) is used:

Relationship (10) $DS=PAW_0-PAW_{n-1}$

In the above relation, PAWO is the amount of rain that is available to the plant's root in n month, and PAWn-1 is also the amount of rain that is available to the plant in a month before the n month. Therefore, using the above quantities, the surplus and the shortage of water are calculated by the relationships (11) and (12):

Relationship (11) $\text{Surplus} = P - AET - DS$

In this regard, Surplus surplus blue, P monthly precipitation, AET actual evaporation and DS changes in soil moisture storage.
Also used to calculate the deficit (Deficit) of (12) is:

Relationship (12) $\text{Deficit} = PET - AET$

3. The study area

The geographical location and political divisions of the Golestan province, with an area of 2.22 km2, are located in the north-eastern part of the country. This province is neighboring with the Caspian Sea (Mazandaran), east of Khorasan province, west with Mazandaran province and south with Semnan province. The average annual rainfall in the watersheds of the province is about 450 mm, so it is about 200 mm in the southern highlands up to 900 mm and in the plains in the north of the province and the border strip. The average annual temperature in the southern regions is about 10 ° C and in the north of the province is up to 17.5 °. The position of the studied basin, Haji Ghoshan, is located in the east of Golestan province in the eastern length of 34º69'90" to 45º33'70" and the northern boundary is 40 º90'90" to 41º84'70". The basin is located east of Khorasan province, south to Semnan and from the north to the Caspian Sea. The monitoring of evapotranspiration by computational methods should be such as to use a method whose climatic components are available at most stations and can be calculated with minimum components for evapotranspiration. Therefore, the Toronto method, based on its calculations based on temperature, may be one of the solutions. But, as mentioned, it can not count on purely computational outputs. Therefore, it is suggested that the evapotranspiration and transpiration rates are calculated using the White Torrent method, if correlated to the experimental data of the mattress with the Torrent White computing data, then its values are corrected by the matched data and based on the regression equation. Therefore, the present study was carried out to calculate the actual evapotranspiration in the Golestan province. One of the eastern catchment areas of the province named Haji Ghoshan basin was selected as the study area. Finally,

the purpose of this study was to calculate the actual evaporation amount using the White Matter Tupert Method and to investigate Critical changes and trends are expected in the future for the study area.

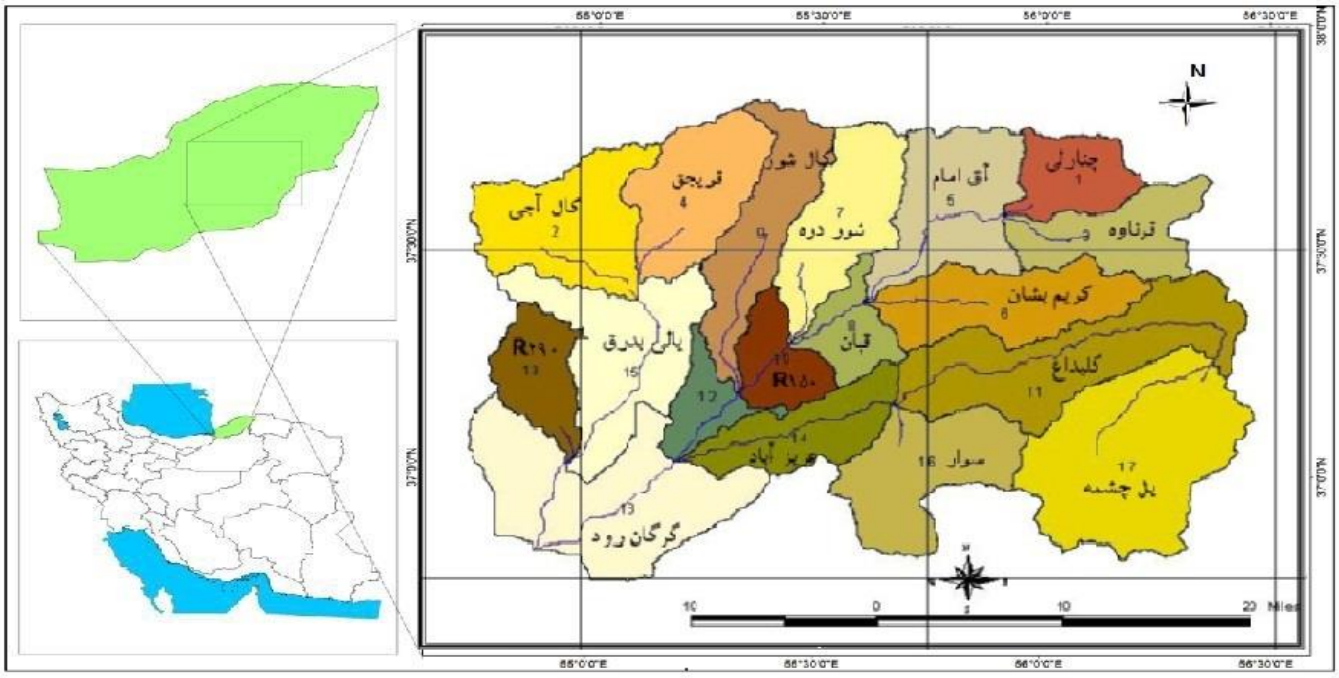

Figure 1. Position of study area

4. Findings

Comparison of actual evaporation variations of the base course with two scenarios RCP 8.5, 4.5

Table 3. Range of actual evaporation changes

RCP4.5(mm)	RCP8.5(mm)	Basic Period (mm)	month
32-95	31-108	42-97	April
18-60	16-63	22-77	May
10-35	9-32	12-35	June
9-30	10-37	12-31	July
11-39	9-34	*15-36*	August
18-49	19-44	20-41	september
22-50	21-47	24-48	october
32-58	28-59	34-61	November
34-54	35-57	32-55	December
27-50	32-52	20-49	January
43-62	44-66	33-63	February
44-79	37-83	49-74	March

RCP8.5 (mm) R

RCP4.5	RCP8.5	Basic Period (mm)	Month
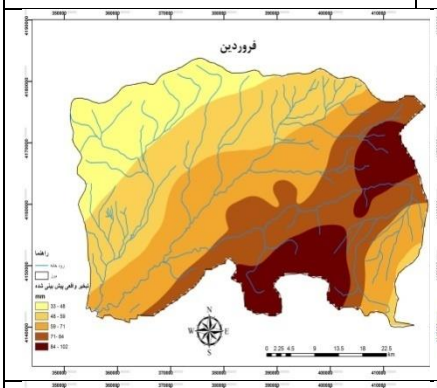	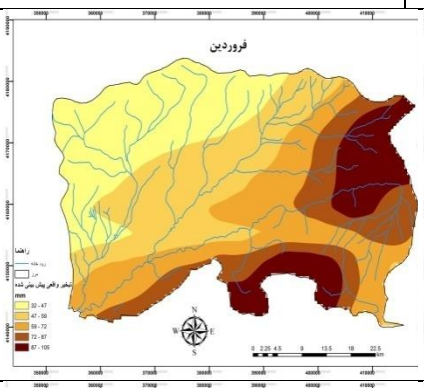	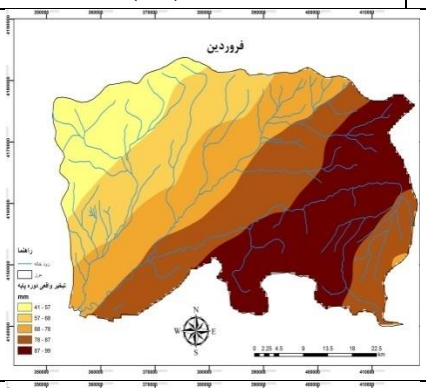	April
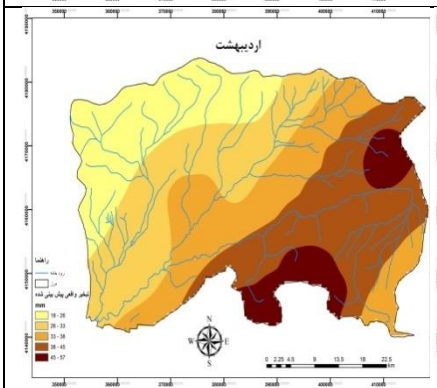	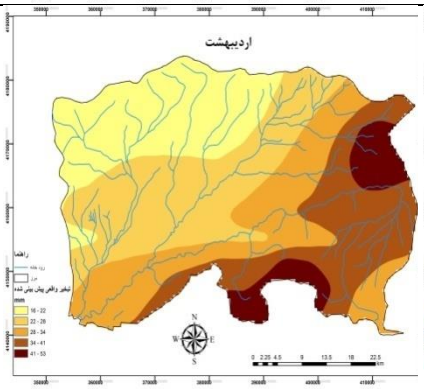	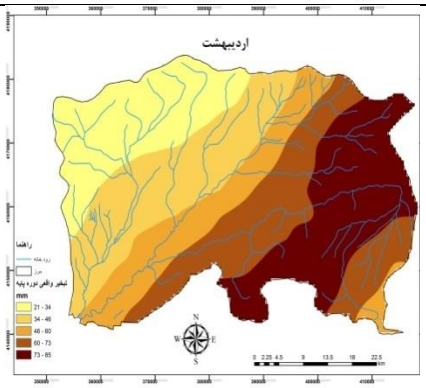	May
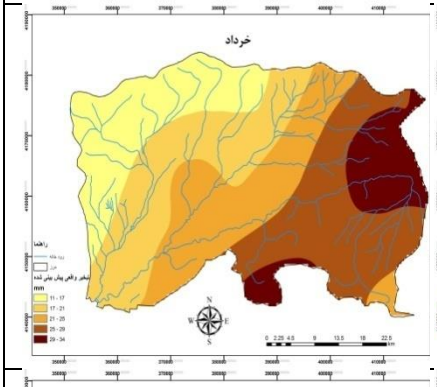	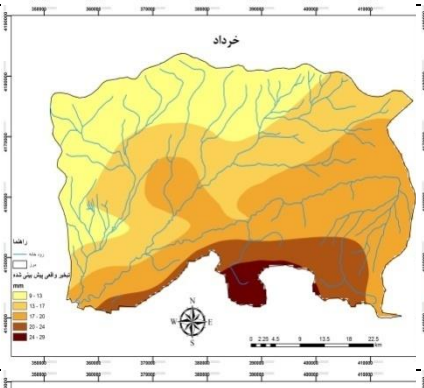	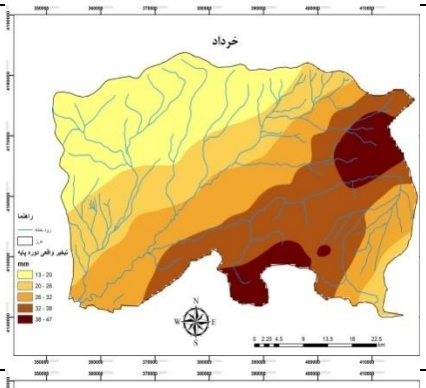	June
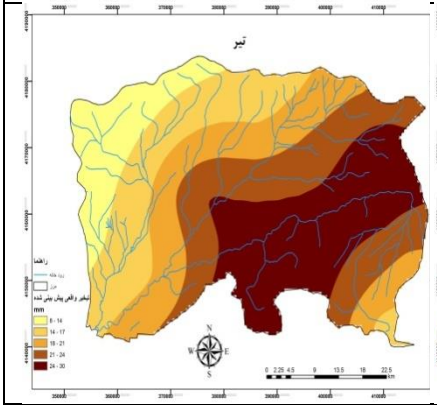	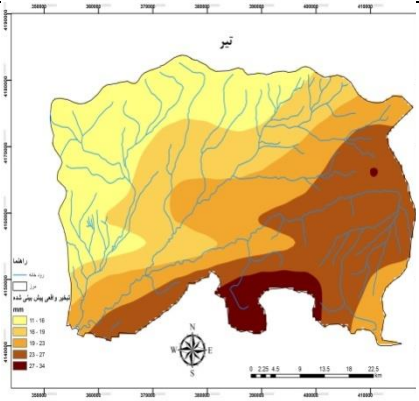	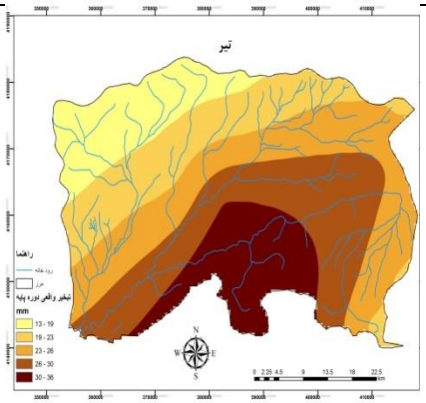	July

RCP4.5	RCP8.5	Basic Period (mm)	month
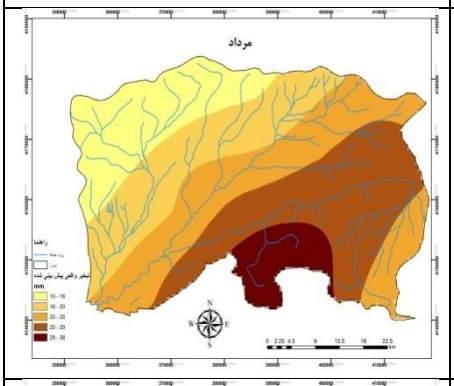	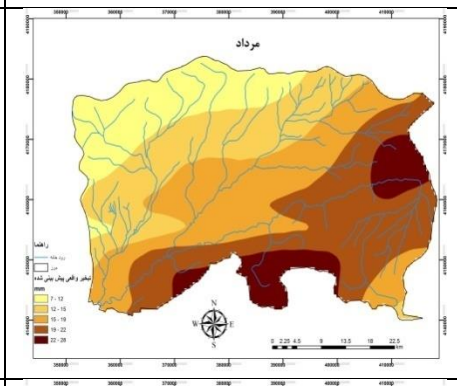	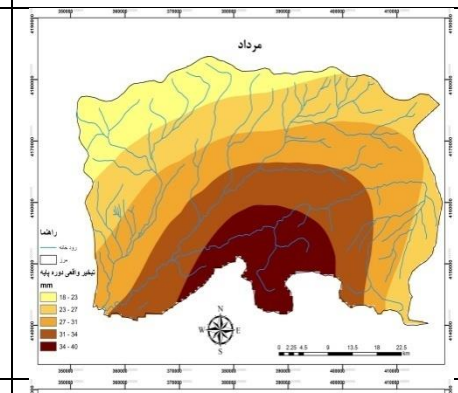	August
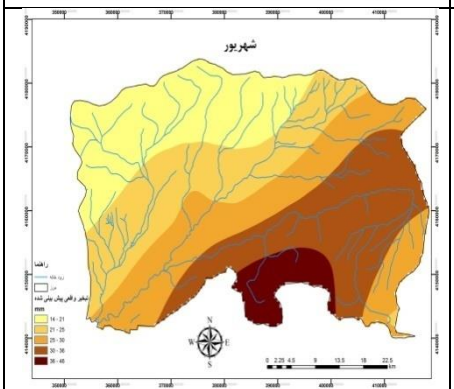	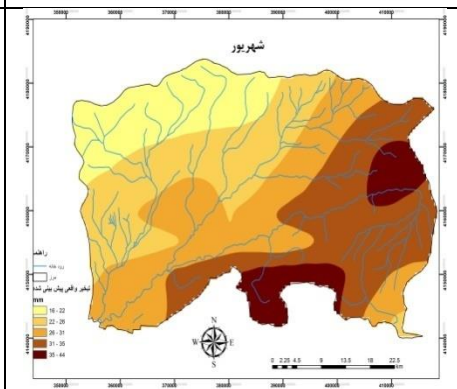	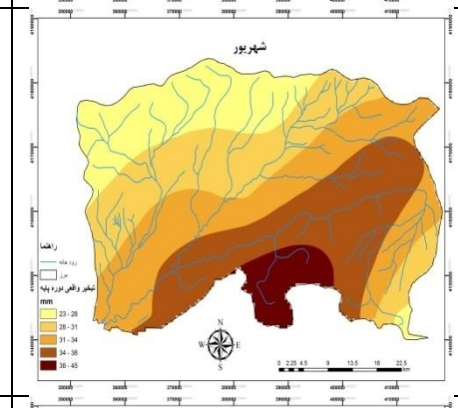	September
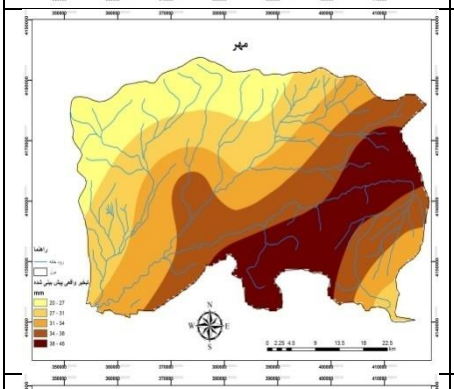	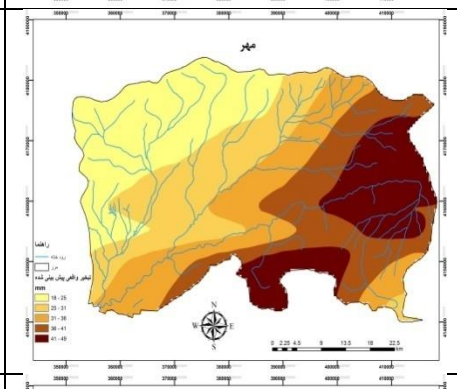	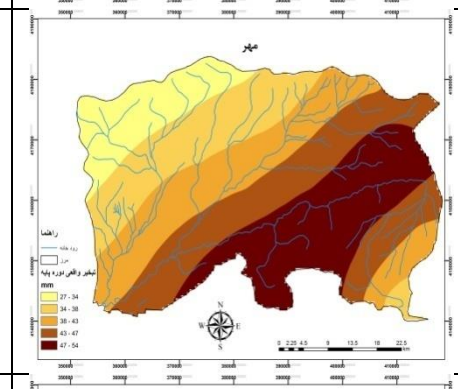	October
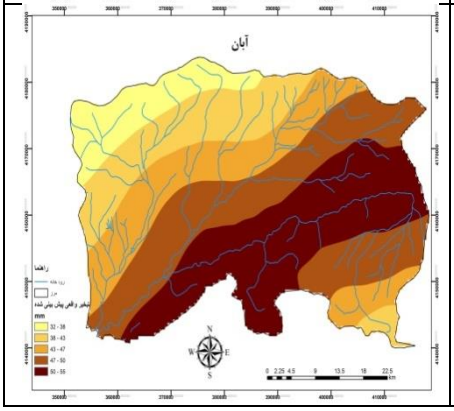	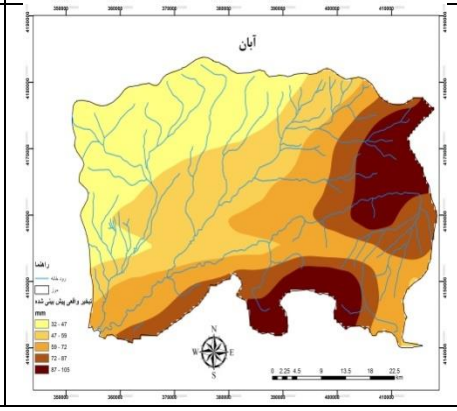	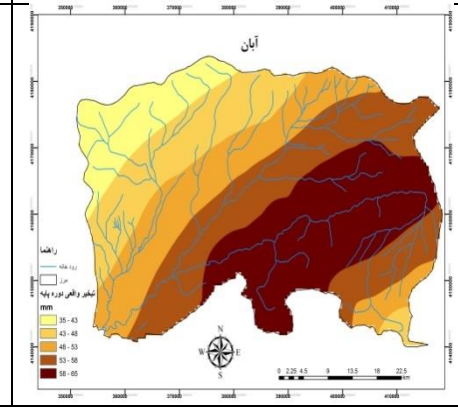	November

RCP4.5	RCP8.5	Basic Period (mm)	month
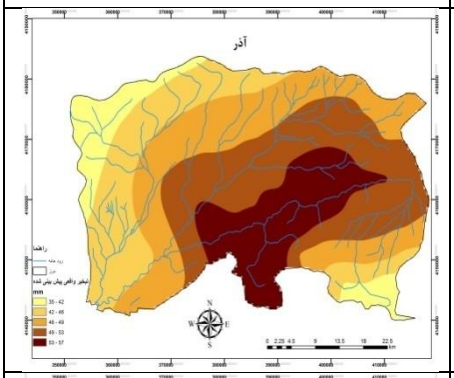	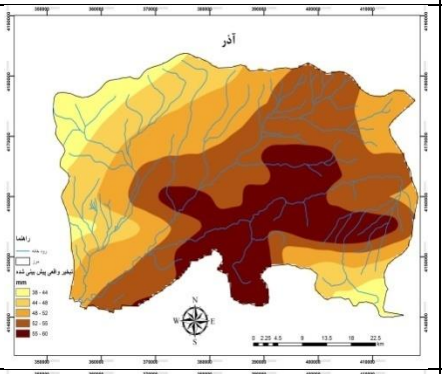	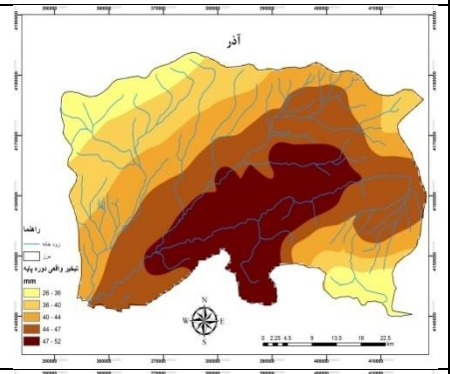	December
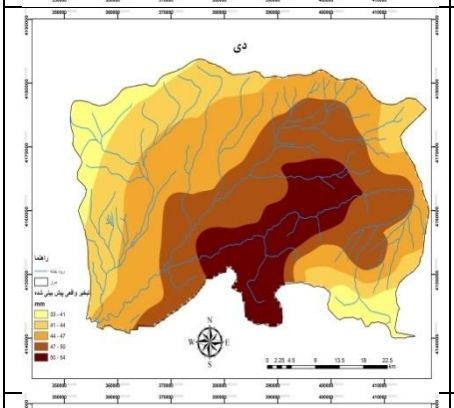	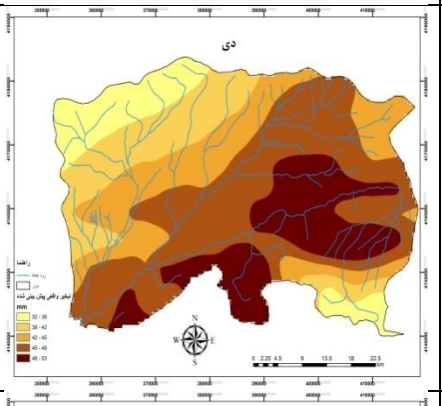	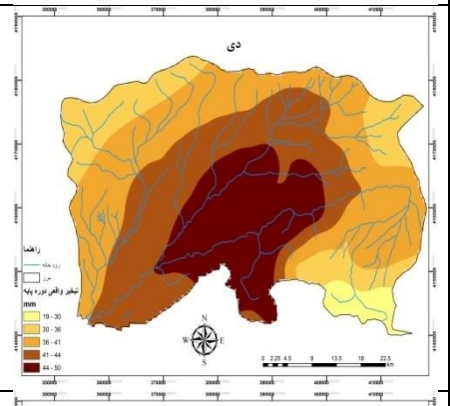	January
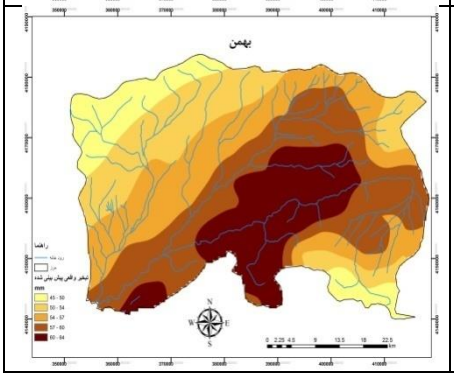	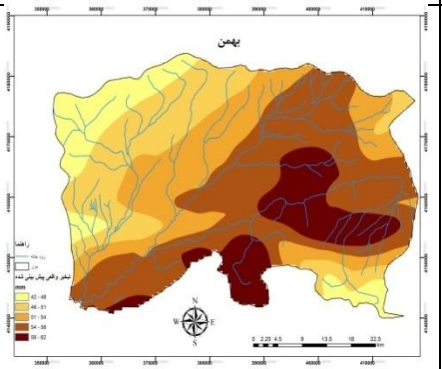	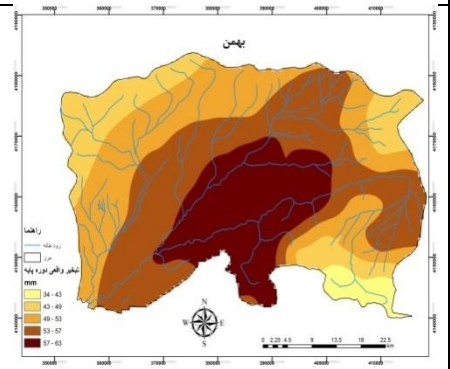	Febrary
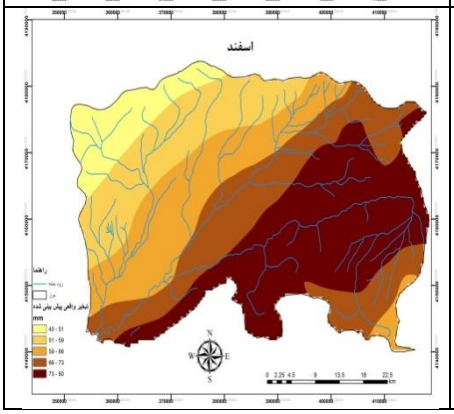	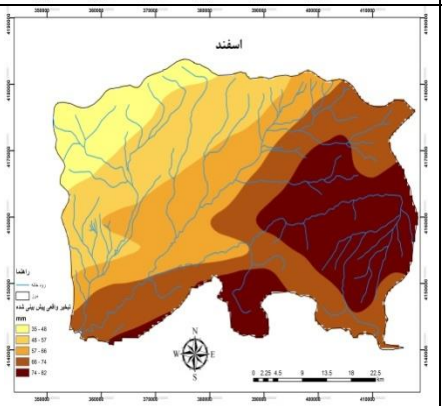	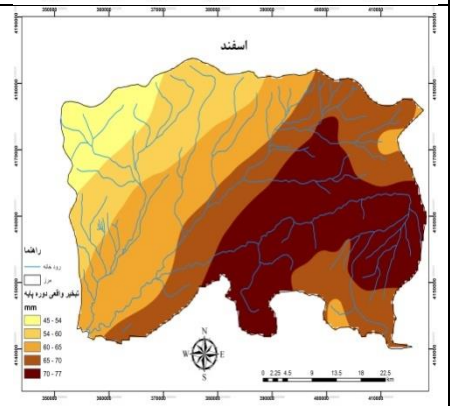	March

rcp4.5.8.5 Figure 2. Comparison of actual evaporation variations of the base course with two scenarios

According to the actual evaporation maps mentioned above, the base maps can be compared with the predicted maps of the two scenarios 8.5 and 4.5. As shown in Table 3, the highest evaporation rate occurred in April. In general, actual evaporation in

the predicted period has increased in two scenarios relative to the base. In all cases, except in April, December and March, the forecast periods will increase compared to the base.

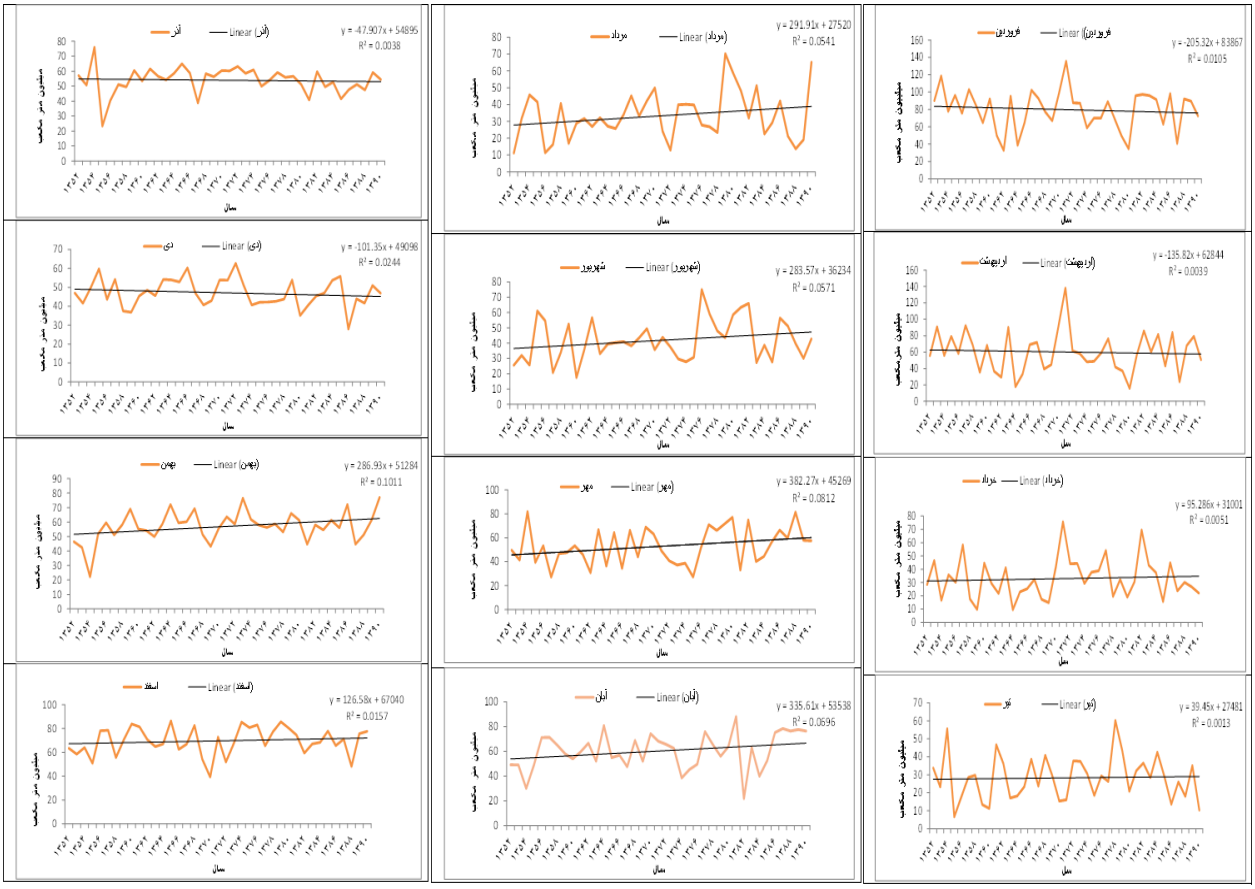

Figure 3. Monthly chart of the actual evaporation variation of the base course

Table 4. Trend of the evolution of the base course changes

R^2	R	Number of observations	month
0.10	0.0105	40	Apri
0.06	0.0039	40	May
0.07	0.0051	40	June
0.03	0.0013	40	July
0.23	0.0541	40	August
0.23	0.0571	40	september
0.28*	0.0812	40	october
0.26*	0.0696	40	November
0.06	0.0038	40	december
0.15	0.0244	40	January
0.31*	0.1011	40	February
0.12	0. 0157	40	March

* According to table 4 of Pearson's significant table, at a 5% error level, a significant range of 0.26 is considered. Only in the months of October, November and February, the coefficient of R^2 is more than 0.26, and their values are similar. Months The trend is not significant. And based on the increasing and decreasing trend, the months of April, June, August, November, December, January, February, March are rising, with only significant changes in November and February. And May, July, September , October, have been decreasing trend among which october month has a significant decreasing trend.

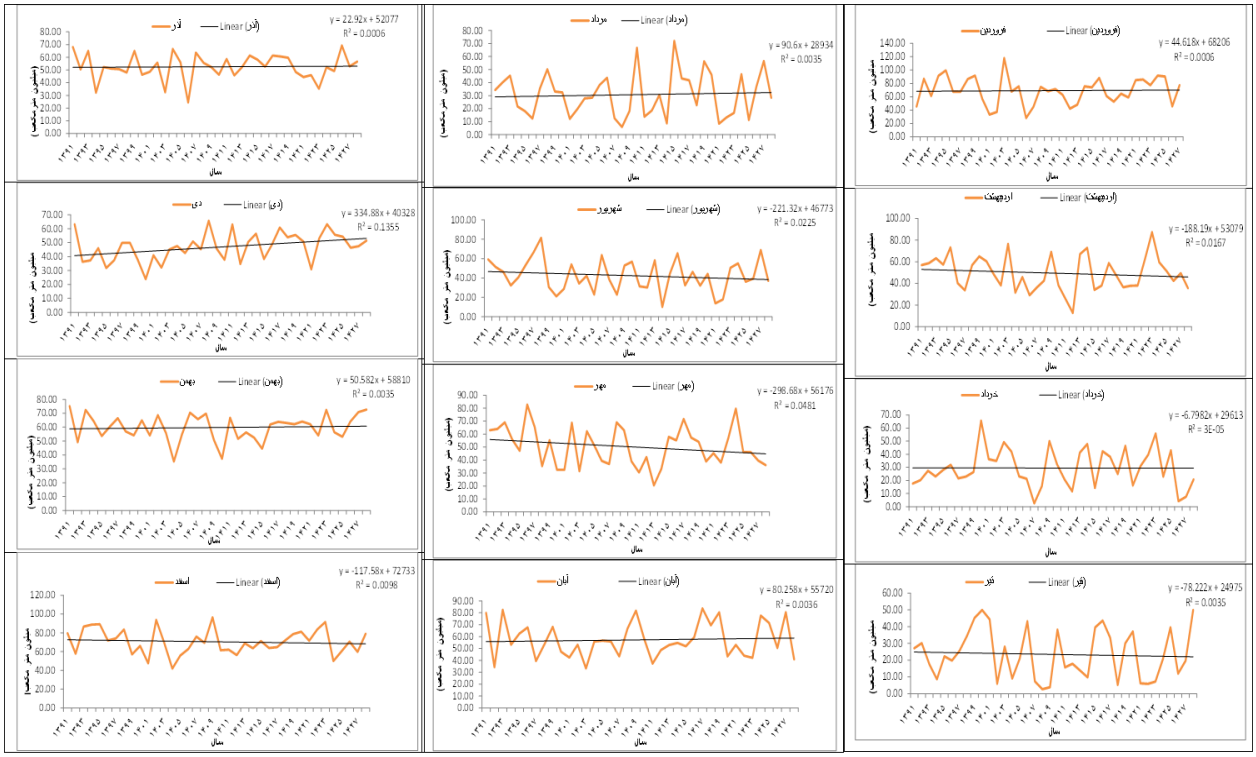

Figure 5. Monthly chart of the evolution of the evolution of the RCP4 scenario

Table 5. The evolution of the evolution of the RCP4 scenario

R^2	R	Number of observations	month
0.024495	0.0006	40	Apri
0.129228	0.0167	40	May
0.022361	0.0005	40	June
0.059161	0.0035	40	July
0.059161	0.0035	40	August
0.15	0.0225	40	september
0.219317	0.0481	40	october
0.06	0.0036	40	November
0. 024495	0.0006	40	december
0.368103*	0.1355	40	January
0.059161	0.0035	40	February
0.098995	0.0098	40	March

* According to Table 5, Pearson's significant table has been found at 5% error level. The domain is considered to be significant at 0.26. The Moon has a coefficient of R2 of more than 0.26 and is significant and has a significant upward trend and other months They will not have meaningful trends.

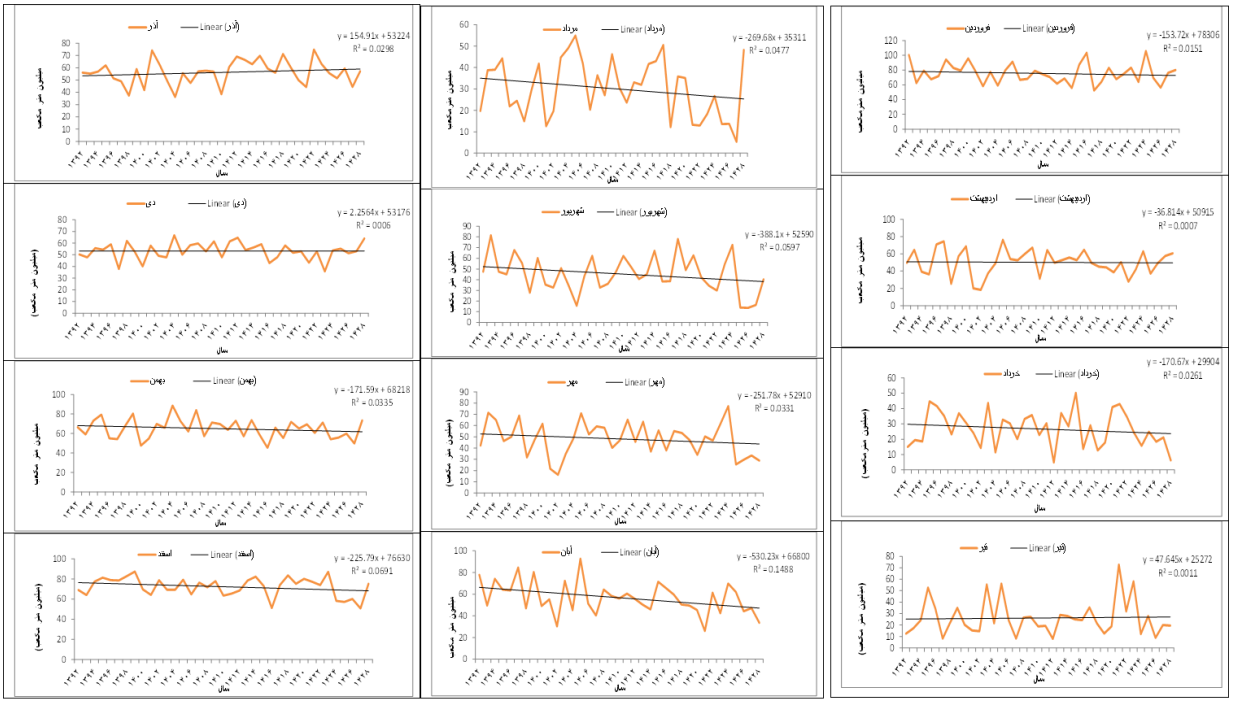

Figure 6. Monthly Chart of the Evolution Chart of the RCP Scenario 8.5

Table 6. The evolution of the evolution of the scenario RCP8.5

R^2	R	Number of observations	month
0.12	0.0151	40	Apri
0.02	0.0007	40	May
0.16	0.0261	40	June
0.03	0.0011	40	July
0.21	0.0477	40	August
0.24	0.0597	40	september
0.18	0.0331	40	october
0.38*	0.1488	40	November
0. 17	0.0298	40	december
0.02	0.0006	40	January
0.18	0.0335	40	February
0.26*	0.0691	40	March

* According to Table 6, Pearson's meaningful table is observed at 5% error rate. The range of 0.26 is considered significant. In the months of November and March, the coefficient of R2 is more than 0.26 and is significant. And each The two have a meaningful downward trend and other months have no meaningful trend.

5. Conclusion

In the present study, studies on the trend of actual evaporation in the Haji Ghoshan watershed and its prediction of the Blue Thoret White script were used with input of the two main components of temperature and precipitation as a component of the variability and considered the other constant component And on the other hand, these two components were displayed using the output of the ESGF-CMIP5 models for future periods of the microscale. Data from the NASA Meteorological Center has been extracted from thredds-ncss-grid-CMIP5. In simulating real evaporation with the Torrent White model, calibration and prediction maps indicate the acceptable performance of this model in estimating actual evaporation in the research area. In the actual evaporation assessment, it was observed that changes under the RCP 8.5 and 4.5 scenario would be followed by a downward trend. Based on the observation that the correlation with the weathering was carried out during the base period, the results showed that the rainfall situation in the basin was relatively better than its future simulation. In the study, in the planning stage, it was observed that the river exploration in the basin studied dependence and direct relation with rainfall Compared to the actual evapotranspiration maps, real evaporation during the base period was more than that of the future simulated situation, as well as in the monthly and yearly trends of the monthly trend for the base period, most of which have experienced an increase in this period, as well as the overall trend of the year There has been an increasing trend for the 40-year period (base course).

Therefore, according to the explanations and results obtained above, it is concluded that during the course of the base the evaporation is increasing. The trend of the monthly currencies trend in the upcoming period in both scenarios 4.5 and 8.5 RCP During this period, the predicted trend for analysts would have a decreasing trend in the scenarios 4.5, months of May, June, July, September, October and March. August, November, December, January and February will have an increasing trend, and the month of April will be a constant trend. But in the 8.5 month scenario, April , June , August , September , October , November January and February will have a decreasing trend of real evaporation. And in the months of July and January, the process of evaporation will increase, and for the month of May, a steady trend is anticipated.

REFERENCES

Mahdavi, Mohammad. (1999). Applied Hydrology "Volume II, Second Edition, Tehran University Press (In Persian).

Shamsipour, Ali Akbar. (2014) Climate Modeling: A Theory and Method ", Tehran University Press (In Persian).

Kaviani, Mohammad Reza Book / Fundamentals of Climate and Surveying /, Publication, 2008(In Persian).

Dr. Alinzadeh, Book of Agriculture and Water, Season of Evaporation and Transmission, 1989(In Persian)

Alizadeh, Amin, (2007) Book of Foundations of Applied Hydrology, Evaporation Season. Publications of Ferdowsi University of Mashhad (In Persian)

Qalam-e-Bakhsh Dash, Milad, (2012) Conceptual Modeling of Water Balance at Basin Scale / Master's thesis. Ferdowsi University of Mashhad (In Persian).

Yaghoobzadeh, Mostafa, Saeed Boroumandesabz, Izadpanah, Zahra Wasidakabli, Hesam, (2015).A paper on the study of the spatial variability of evapotranspirational temperature by means of measuring rainfall in semi-arid areas (In Persian).

Ghalizadeh Alpavut, Hamid, AminiNia, Karim (2014) Review of the changes in the potential evapotranspiration time in Tabriz (In Persian).

Ahmadi, Maryam, Farhadi Banseleh, Bahman (2011) the Temporal and Spatial Changes of Coefficient of Evaporation in Kermanshah Province (In Persian).

Seyfi, Akram, Riahi Madvar, Hussein (2016) "A Survey of Sudden Changes and Pattern of Perspective Evapotranspiration Change Patterns by Wavelet Analysis and Mobile T-Test"(In Persian).

Miriqoubzadeh, Mir Hossein. Soleimani, Karim. Habibnejad Bright, Mahmoud, Kaka Shahedi. Abbaspour, Karim. Brotherhood, Samira,(2013). "Determination and Evaluation of Real Evapotranspiration Using Remote Sensing Data; Case Study of Sour Watershed, Golestan" (In Persian).

Reza Ebrahimi,(2013)Iran's Comprehensive Climate and Weather Climate website(In Persian).

Bastiaanssen, W.G.M. (2000). SEBAL-based sensible and latent heat fluxes in the irrigated Gediz BasinTurkey, 229, 87–100

Su, H., E.F. Wood, R. Wojcik & M. McCabe. (2006). Sensitivity Analysis of Regional Scale Evapotranspiration Predictions to the Forcing Data, American Geophysical Union, Fall Meeting2007, abstract #H31A-02.

Teixeira, A.H., W.G.M. Bastiaanssen, M.D. Ahmad & M.G. Bos. 2009. Reviewing SEBAL input parameters for assessing evapotranspiration and water productivity for the Low-Middle Sao Francisco River basin, Brazil Part A: Calibration and validation, agricultural and forest meteorology, 149, 462-76.

Yang, J., Reichert, P., Abbaspour, K.C., and Yang, H. (2007), Hydrological modelling of the Chaohe Basin in China: Statistical model formulation and Bayesian inference. Journal of Hydrology, 340:167–182.

Sawano, Shinji, Hotta, Norifumi, Komatsu, Hikaru, Suzuki, Masakazu and Yayama, Tomoko.(2007)" Forest Environments in the Mekong River Basin (Evaluation of Evapotranspiration in Forested Areas in the Mekong Basin Using GIS Data Analysis", Pp: 295 (36-44).

Lin, Chih-Hsien, Chao, Cheng and Chen, Wen-Fu, 2008, Estimation Regional Evapotranspiration by Adaptive Network-based Fuzzy Inference System for Dan-Shui Basin in Taiwan, J. Chinese Inst. of Eng. 30(6): 1091-1096.

George, Paul, Prasanna, H. Gowda, P.V. Vara, Prasad, Terry A. Howell, Scott A. Staggenborg, Christopher M.U. Neale(2013), Lysimetric evaluation of SEBAL using high resolution airborne imagery from BEAREX08, Advances in Water Resources, in press.

Jacobs,J.M., Mergelsberg,S.L., Lopera,A.F and Myers,D.A. 2002. Evaporation from a wet prairie wetland under conditions. Paynes Prairie Preserve.